文章编号：1001-9014(2020)05-0547-06

DOI:10. 11972/j. issn. 1001-9014. 2020. 05. 003

Detailed investigations on double confocal waveguide for a gyro-TWT

ZHANG Chen, WANG Wei, SONG Tao, HUANG Jie, CAO Yi-Chao, LIU Di-Wei*, HU Min, ZHANG Kai-Chun, WU Zhen-Hua, ZHOU-Jun , ZHONG Ren-Bin, ZHAO Tao, GONG Seng, LIU Sheng-Gang

(Terahertz Research Center, School of Electronic Science and Engineering, University of Electronic Science and Technology of China, Chengdu 610054, China)

Abstract: The electromagnetic characteristics of the double confocal waveguide for a gyro-TWT is investigated in details. The eigenvalue and the field distribution of two kinds of steady-state modes in a double confocal waveguide, namely the superposition mode and the ring mode, are calculated with the scalar formulation of Huygens' Principle, the theoretical results agree well with those from the commercial CST software. When the anti-phase superposition mode TE_{06} mode is chosen as an operating mode in a gyro-TWT, the diffractive loss of the potential parasitic modes is far greater than that of the operating mode. It means that the potential parasitic modes can be suppressed by means of its own diffractive loss in a double confocal waveguide. The mode density in a double confocal waveguide is higher than that in a single confocal waveguide, but far lower than that in a cylindrical waveguide. Compared to the single confocal waveguide, a higher beam-wave interaction efficiency can be obtained in the double confocal waveguide for a gyro-TWT, it is an appropriate choice to choose a double confocal waveguide as the beam-wave interaction structure in a gyro-TWT.

Key words: double confocal waveguide, gyro-TWT, Terahertz, superposition mode, ring mode

PACS: : 84. 40. Az

双共焦波导回旋行波管高频结构的电磁特性研究

张 晨, 王 维, 宋 韬, 黄 杰, 曹毅超, 刘颋威*, 胡 旻, 张开春, 吴振华, 周 俊, 钟任斌, 赵 陶, 龚 森, 刘盛纲

(电子科技大学 电子科学与工程学院 ,太赫兹研究中心,四川 成都 610054)

摘要:研究了双共焦波导回旋行波管高频结构的电磁特性。根据惠根斯原理的光衍射理论,分析得出双共焦波导中的两类本征模式(叠加模和环形模)对应的截止频率和场分布情况。理论分析结果与商用仿真软件CST的仿真结果一致。其中用作回旋行波管工作模式的"反相叠加TE_{06}模"的损耗明显小于其他模式,这种不同模式损耗不同的特性将有效抑制竞争模式带来的寄生振荡。双共焦波导的模式密度略大于传统单共焦波导的模式密度,但是明显小于圆波导的模式密度,因此双共焦波导适合用作回旋行波管的高频结构。

关 键 词:双共焦波导;回旋行波管;太赫兹;叠加模;环形模

中图分类号:TN128 **文献标识码**:A

Introduction

High average-power gyrotron traveling-wave tubes (gyro-TWT) have abroad applications in modern communication and radar systems[1-3]. Conventional gyro-TWT can operate at Ka and W band with high output power, but they face significant obstacles in extension to operate at higher frequency with high average power. The reason is that these devices utilize the fundamental or low-order modes of the interaction structure to avoid mode competition; the power capability and ohmic loss in such small structures are inevitable to limit the average power at high frequency. In 2003, a single confocal waveguide gy-

Received date: 2019-12-21, **revised date**: 2020- 05- 27 **收稿日期**:2019-12-21,**修回日期**:2020- 05- 27

Foundation items: Supported in part by the National Key Research and Development Program of China under Grant 2017YFA0701000, in part by the Natural Science Foundation of China (61988102) and the Fundamental Research Funds for the Central Universities under (A03018023601003).

Biography: ZHANG Chen (1995-), male, Chengdu, China, doctor. Research area involves terahertz technology and applications. E-mail: 2932433214@qq. com.

* **Corresponding author**: E-mail: dwliu212220@163. com

ro-TWT has been proposed by MIT. This quasioptical mode-selective interaction structure allows a stable single-mode operation in the overmoded interaction structure at high frequency and high power [4-6].

The drawback of the gyro-TWT with a single confocal structure is the relatively low beam-wave interaction efficiency because the conventional annular electron beam is located in the region with different strength of the coupling to the operating mode. One of the possible solutions for mitigating this drawback is to use a double confocal structure. A double confocal waveguide consists of two identical but perpendicular single confocal waveguides in x and y direction, respectively, as shown in Fig. 1. The transverse field distribution in a double confocal waveguide is more uniform than that in a single confocal waveguide, so the conventional thin annular electron beam can interact more efficiently with the RF field in a double confocal waveguide. The theoretical analysis and PIC simulation confirmed that the beam-wave interaction efficiency increases obviously in a double confocal waveguide [7-8].

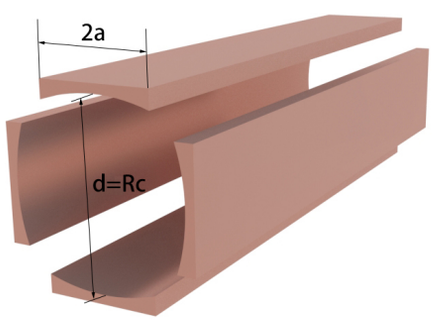

Fig. 1 3-D configuration of a double confocal waveguide
图1 双共焦波导的3维结构

In order to utilize a double confocal waveguide as a beam-wave interaction structure in a gyro-TWT, it is necessary to make clear the eigenmodes and their corresponding electromagnetic (EM) characteristics in a double confocal waveguide. In this paper, the EM characteristics of a double confocal waveguide for a gyro-TWT will be investigated in details. The rest of this paper is organized as following. The investigation on eigenmodes in a double confocal waveguide is presented in section 1, in section 2, the diffraction loss is discussed. Summary and conclusion are presented in section 3.

1 Eigenmodes of a Double Confocal Waveguide

The double confocal waveguide is an open structure formed by four identical symmetrically placed curved cylindrical mirrors, in which four mirrors with a radius of R_c and a mirror width of $2a$ are separated with a distance of d. EM wave is reflected among mirrors. There are two kinds of stable modes with different reflection paths in a double confocal waveguide. The first steady-state mode, namely, the superposition mode, is superposed by two perpendicular in-phase or anti-phase field, as shown in Fig. 2(a). The second steady-state mode, namely, the ring mode, is formed by the consecutive reflection of the field among four mirrors in clockwise or counterclockwise directions, as shown in Fig. 2(b).

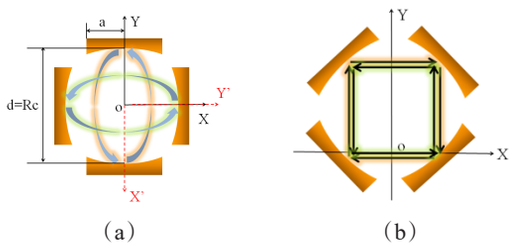

Fig. 2 The diagram of the modes in a double confocal waveguide (a) Superposition mode; (b) Ring mode
图2 双共焦波导中两类模式的构成形式(a)叠加模的构型;(b)环形模的构型

All resonator dimensions are assumed large compared to a wavelength; the eigenmodes of the resonator are therefore obtainable from a self-consistent field analysis using Huygens' Principle. The Fresnel field U_p at the point of observation is given by the surface integral [9]

$$U_p = \frac{jk}{4\pi}\iint_A U_a \frac{e^{-ik\rho}}{\rho}(1+\cos\theta)\,dS \quad , \quad (1)$$

where k is the propagation constant, ρ is the distance from a source point on the mirror to the point of observation and θ is the angle between ρ and the normal of the source point.

1.1 Superposition modes

For a superposition mode, which is superposed by two perpendicular standing wave in x and y direction, respectively, and the eigensolution of the standing wave is as follows. In Fig. 3, the field $U_2(x_2)$ on mirror S_2 can be obtained in term of an integral of the known field $U_1(x_1)$ on mirror S_1 in y direction with eq. (1).

$$U_2(x_2) = \sqrt{\frac{jk}{2\pi d}}\iint_A U_1(x_1)\,e^{-ik\rho}\,dS_1 \quad . \quad (2)$$

The eigenfunctions of the modes in a confocal waveguide can be obtained by making sure that the field distribution over S_1 can reproduce itself with a constant over

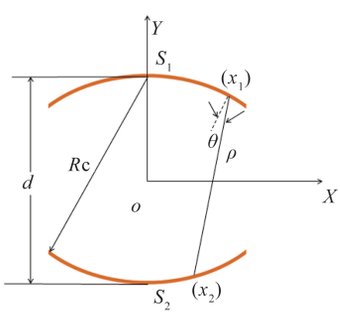

Fig. 3 Confocal waveguide with spherical reflectors
图3 单共焦波导横截面几何结构图

S_2, namely, $U_2(x_2) = b_m U_1(x_1)$, where b_m is general complex, including both the amplitude and phase changes. In this case, eq. (2) can be rewritten as following

$$b_m U_1(x_1) = \sqrt{\frac{jk}{2\pi d}} \iint_A U_1(x_1') e^{-ik\rho'} dS_1' \quad , \quad (3)$$

with

$$\rho' = d - x_1 x_1' / d \quad . \quad (4)$$

For this general solution, the eigenvalues can be expressed as $b_m = \exp(-p_m - ikd + i\Delta_m)$. The amplitude of b_m is related to the diffraction loss, and the phase of b_m determines the phase shift of the mode from S_1 to S_2, where kd is the geometric phase shift and Δ_m is the additional phase shift. The phase shift of a complete field reflection in the cross section of the resonator must be an integer n times of 2π, namely. $kd - \Delta_m = n\pi$. By solving eq. (3), the cut-off wavenumber of the superposition mode can be written as

$$k_t = \frac{\pi}{d}\left(n + \frac{m}{2} + \frac{1}{4}\right) \quad . \quad (5)$$

The field between S_1 and S_2 can be calculated based on Huygens' Principle as presented in eq. (1). Approximately, the field distribution between S_1 and S_2 can be considered as a superposition of two Gaussian beams. The membrane function of standing wave (superposition of two Gaussian beams) can be written as [10-11]:

$$\Psi_{mn}(x,y) = \sqrt{\frac{w_0}{w(y)}}\, \phi_m\left[-\frac{\sqrt{2}\,x}{w(y)}\right] \times \begin{cases} \cos\xi, n = 2, 4, 6, \ldots \\ \sin\xi, n = 3, 5, 7, \ldots \end{cases} \quad , \quad (6)$$

where

$$\zeta = \frac{k_t x^2}{2R(y)} + k_t y - \left(m + \frac{1}{2}\right)\arctan\frac{2y}{k_t w_0^2} \quad , \quad (7)$$

$$R(y) = y\left[1 + \left(\frac{kw_0^2}{2y}\right)^2\right], w(y) = w_0\sqrt{1 + \left(\frac{2y}{kw_0^2}\right)^2} \quad , \quad (8)$$

$$\phi_m(\tau) = H_m(\tau)\exp\left(-\tau^2/2\right) \quad , \quad (9)$$

here, $H_m(\tau)$ is the Hermite polynomial and $w_0^2 = d/k_t\sqrt{2R_c/d - 1}$.

Similarly, the field distribution between two mirrors in x direction can be calculated in the same way. The superposition mode can be considered as a liner superposition of two in-phase or anti-phase standing waves, and the membrane function can be expressed as following:

$$\begin{aligned} \Psi_{mn}^{in}(x,y) &= \Psi_{mn}(x,y) + \Psi_{mn}(-y,x) \\ \Psi_{mn}^{anti}(x,y) &= \Psi_{mn}(x,y) - \Psi_{mn}(-y,x) \end{aligned} \quad , \quad (10)$$

where $\Psi_{mn}(x,y)$ has been expressed in eq. (6). With the membrane functions $\Psi_{mn}^{in}(x,y)$ and $\Psi_{mn}^{anti}(x,y)$ of the superposition modes in a double confocal waveguide, by solving the Maxwell's equations in a Cartesian coordinate system, the field components of TE_{mn} mode can be obtained.

The magnitude of the transverse electric field of the superposition mode in a double confocal waveguide is presented in Fig. 4. Fig. 4 (a), (b), (c) and (d) are the field of the superposition TE_{06}^{in}, TE_{06}^{anti}, TE_{15}^{in} and TE_{15}^{anti} modes simulated by commercial CST software, the theoretical results of the field are presented in Fig. 4 (e), (f), (g) and (h). The theoretical results agree well with those obtained by the commercial CST software. It is worth noting that the theoretical calculation only includes the central area surrounded by the mirror, and the diffraction field between the mirrors is not included in the theoretical calculation.

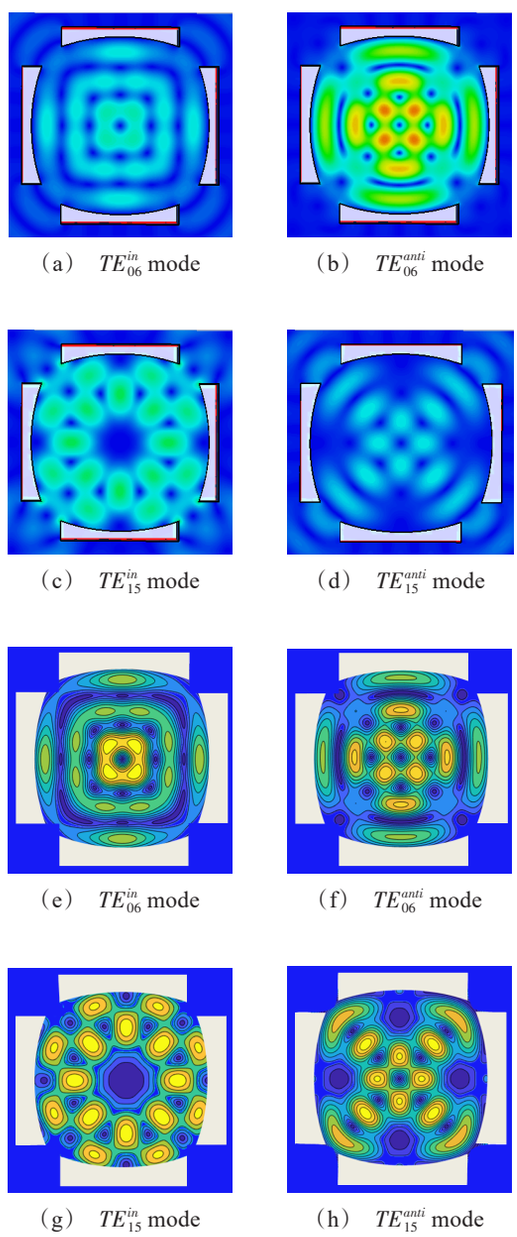

(a) TE_{06}^{in} mode　(b) TE_{06}^{anti} mode

(c) TE_{15}^{in} mode　(d) TE_{15}^{anti} mode

(e) TE_{06}^{in} mode　(f) TE_{06}^{anti} mode

(g) TE_{15}^{in} mode　(h) TE_{15}^{anti} mode

Fig. 4　The magnitude of electric field of the superposition modes in a double confocal waveguide (a), (b), (c) and (d) are the results simulated by commercial CST software; (e), (f), (g) and (h) are the theoretical results.: (a), (b), (c)和(d)是仿真软件CST的计算结果, (e), (f), (g)和(h)是理论计算结果

图4　双共焦波导部分叠加模横向电场幅值分布图

In the Cartesian coordinate system, the coupling factor (Form factor) characterizing the Lorentz force on electrons can be expressed as[2]

$$L_s = \left| \frac{1}{2\pi} \int_0^{2\pi} \frac{1}{k_t} \left(\frac{\partial}{\partial X} + \mathrm{i} \frac{\partial}{\partial Y} \right) \Psi_{mn}(X,Y)\, d\theta \right|^2 , \quad (11)$$

$$X = r_b \cos(\theta), \quad Y = r_b \sin(\theta) , \quad (12)$$

Fig. 5 presents the normalized beam-wave coupling factor of the double confocal mode TE_{06}^{anti} and the single confocal modeTE_{06} versus the guiding center radius R_b, and the beam-wave coupling factor in a double confocal waveguide is greater than that in a single confocal waveguide.

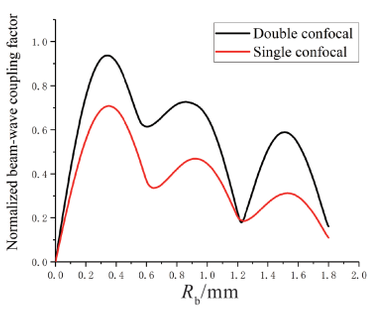

Fig. 5 Normalized beam-wave coupling coefficient versus R_b.
图5 归一化的注-波耦合系数随波导半径的变化

1.2 Ring modes

The other kind of mode in a double confocal waveguide is the ring mode. The ring mode is formed by the consecutive reflection among four mirrors in clockwise or counterclockwise directions.

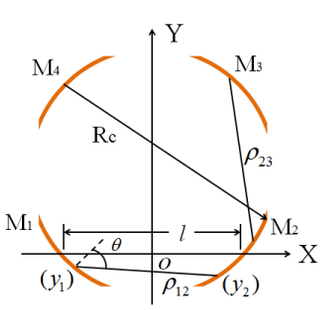

Fig. 6 Coordinate systems for the ring mode
图6 环形光学谐振腔横截面几何结构图.

Based on the scalar formulation of Huygens' Principle in eq. (1), if we know the field distribution $U_1(y_1)$ on mirror M_1, we can calculate the field $U_2(y_2)$ on mirror M_2. Then, the field $U_2(y_2)$ is reflected to M_3 in the same way to form $U_3(y_3)$. It is conceivable that after multiple reflections the field will eventually reach a steady state. $U_3(y_3)$ and $U_1(y_1)$ satisfy the following relationship: $U_3(y_2) = b_m U_1(y_1)$. The resulting integral equation is presented as follows

$$b_m U_1(y_1) = \iint_{M_2} dS_2 \iint_{M_1} dS_1 K_{12} K_{23} U_1(y_1') , \quad (13)$$

In eq. (13), K_{mn} are defined as

$$K_{mn} = \sqrt{\frac{jk\cos\theta}{2\pi}} \frac{e^{-jk\rho_{mn}}}{\rho_{mn}} , \quad (14)$$

where ρ_{mn} represents the distance between any two points on mirror M_m and mirror M_n[12].

$$\rho_{mn} = l + y_m y_n \cos^2\theta / l + (y_m - y_n)\sin\theta - (y_m^2 + y_n^2)\cos^2\theta \left[(l - R_c\cos\theta) / 2lR_c\cos\theta \right], \quad (15)$$

For this general solution, the eigenvalues can be expressed as$b_m = \exp(-p_m - i2kl + i\Delta_m)$. By solving eq. (13), the cutoff wavenumber of the ring mode TE_{0n} can be written as

$$k_t = \frac{\pi}{2l}\left(n + \frac{3}{2\pi}\right) , \quad (16)$$

where n is an integer for the mode index which represents the number of maxima from M_1 to M_3. The electric field at arbitrary point between M_1 and M_2 can be obtained by calculating the integral of eq. (1) with $U_1(y_1)$ presented in eq. (13).

The field distribution between two adjacent mirrors also can be considered as a standing-wave field formed by the superposition of Gaussian beams propagating clockwise and counterclockwise. The expression of the membrane function of the ring mode can be written as:

$$\Psi_{0n}^{ring}(x,y) = \Psi_{0n}\left(x - \frac{Rc}{2\sqrt{2}}, y\right) + \Psi_{0n}\left(x + \frac{Rc}{2\sqrt{2}}, y\right) + \Psi_{0n}\left(-y + \frac{Rc}{2\sqrt{2}}, x\right) + \Psi_{0n}\left(-y - \frac{Rc}{2\sqrt{2}}, x\right), \quad (17)$$

where $\Psi_{0n}(x, y)$ has been expressed in (6).

The transverse field distribution of the ring modes is shown in Fig. 7. Fig. 7 (a) and (b) is the simulation result of the field distribution from CST, Fig. 7 (c) and (d) is the theoretical calculation result. The theoretical results agree well with those obtained by the commercial CST software.

1.3 Mode density

Table I gives the cutoff frequency of the modes whose cutoff frequency is around 263GHz in a double confocal waveguide with R_c=3.6mm and a=1.2mm. Clearly, the cutoff frequencies of the superposition mode and the ring mode calculated by eqs. (5) and (16) agree well with the simulation results from CST.

The mode densities in a double confocal waveguide, in a single confocal waveguide and in a cylindrical waveguide are presented in Fig. 8, it is obvious that the mode density in a double confocal waveguide is higher than that in a single confocal waveguide, but less than that in a cylindrical waveguide. This is because there are more stable paths for the modes in a double confocal waveguide than in a single confocal waveguide. In addition, the in-phase superposition mode and the anti-phase superposition mode are the degenerate mode, so only one curve is used to represent these two modes in Figure 8(c).

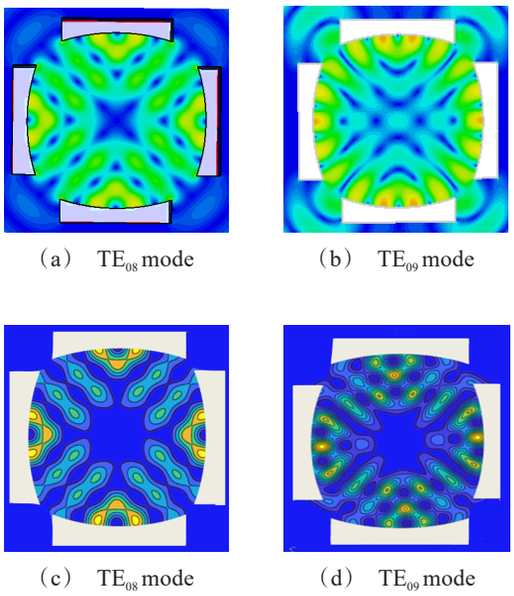

Fig. 7　The magnitude of the electric field of the ring mode, (a) and (b) are the results from the commercial CST software; (c) and (d) are the theoretical results.: (a), (b)是仿真软件CST的计算结果, (e), (f)是理论计算结果
图7　双共焦波导部分环形模横向电场幅值分布图

Table 1　Cut-off frequency of Eigenmodes
表1　各本征模的截止频率

Mode	Theoretical	Simulation
TE_{09} (ring mode)	279. 2 GHz	277. 8 GHz
TE_{06} (superposition mode)	260. 4 GHz	260. 1GHz
TE_{08} (ring mode)	249. 8 GHz	249. 5GHz
TE_{15} (superposition mode)	239. 6 GHz	237. 2 GHz

2　Diffraction losses

For a double confocal waveguide, it is possible to diffract part of power out of the waveguide by means of the gaps among the mirrors; it is helpful against the parasitic oscillation in a gyro-TWT. Table II gives the diffractive loss of different modes in a double confocal waveguide with R_c=3. 6mm and a=1. 2mm. It is found that the diffractive loss of the anti-phase superposition mode TE_{06} mode is far less than that of the potential parasitic modes.

Fig. 9 shows the effect of the gap size on the diffraction losses of the anti-phase superposition mode TE_{06} mode, which is expected to be the operating mode of the Gyro-TWT.

3　Conclusion

The electromagnetic characteristics of the double confocal waveguide for a gyro-TWT is investigated in details. There are two kinds of steady-state modes in a double confocal waveguide, namely, the superposition mode and the ring mode. The superposition mode includes in-phase and anti-phase superposition mode. With the scalar formulation of Huygens' Principle, the eigenvalue and the field distribution of these two kinds of modes

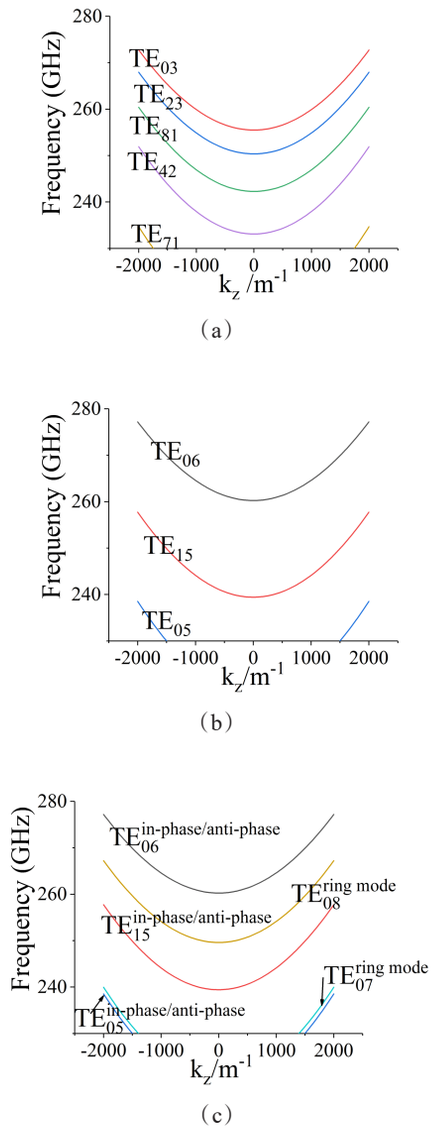

Fig. 8　Dispersion curve. (a) Dispersion curve in a cylindrical waveguide. (b) Dispersion curve in a single confocal waveguide. (c) Dispersion curve in a double confocal waveguide.
图8　波导色散曲线 (a)圆波导的色散曲线(b)单共焦波导的色散曲线(c)双共焦波导的色散曲线

Table 2　Total loss
表2　总的传输损耗

Mode	Total Loss (dB/cm)	Interaction
TE_{09} (ring mode)	28. 2dB	Forward
TE_{06} (in-phase superposition mode)	17. 8	Forward
TE_{06} (anti-phase superposition mode)	2. 03	Forward
TE_{08} (ring mode)	13. 9	BWO
TE_{15} (in-phase superposition mode)	4. 8	BWO
TE_{15} (anti-phase superposition mode)	30. 1	BWO

have been calculated, and the theoretical calculation results agree well with those from the commercial CST soft-

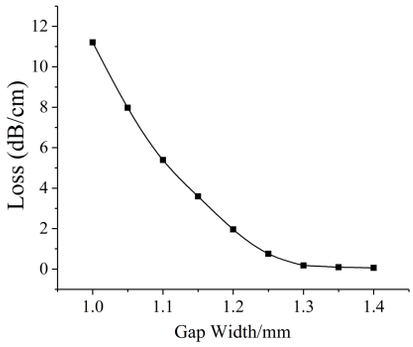

Fig. 9 Variation of diffraction losses of the anti-phase superposition mode TE_{06} mode with the aperture size.
图9 反相叠加TE06模在不同镜宽下的衍射损耗情况

ware. Meanwhile, the diffractive loss has also been calculated with CST software. If the anti-phase superposition mode TE_{06} mode is chosen as an operating mode in a gyro-TWT, the diffractive loss of the potential parasitic modes, such as the ring mode TE_{08} and TE_{09} modes, the superposition mode TE_{06} (in-phase) TE_{15} (in-phase and anti-phase) modes is far greater than that of the operating mode. It means that the potential parasitic modes can be suppressed effectively by means of its own diffractive loss in a double confocal waveguide. The mode density in a double confocal waveguide is higher than that in a single confocal waveguide, but far lower than that in a cylindrical waveguide. Compared to the single confocal waveguide, a higher beam-wave interaction efficiency can be obtained in a double confocal waveguide for a gyro-TWT, it is an appropriate choice to choose a double confocal waveguide as the beam-wave interaction structure in a gyro-TWT.

References

[1] Chu K R. Overview of research on the gyrotron traveling-wave amplifier [J]. *Plasma ence IEEE Transactions on*, 2002, **30**(3):903-908.
[2] Nusinovich G S, Li H. Theory of gyro-travelling-wave tubes at cyclotron harmonics [J]. *International Journal of Electronics*, 1992, **72**(5):895-907.
[3] Chu K R, Chen H Y, Hung C L, *et al*. Ultrahigh Gain Gyrotron Traveling Wave Amplifier [J]. *Physical Review Letters*, 1998, **81**(21):4760-4763.
[4] Sirigiri J R, Shapiro M A, Temkin R J. High-Power 140-GHz Quasi-optical Gyrotron Traveling-Wave Amplifier [J]. *Physical Review Letters*, 2003, **90**(25):258302.
[5] Soane A V, Shapiro M A, Jawla S, *et al*. Operation of a 140-GHz Gyro-Amplifier Using a Dielectric-Loaded, Severless Confocal Waveguide [J]. *IEEE Transactions on Plasma ence IEEE Nuclear & Plasma ences Society*, 2017, **45**(10):2835.
[6] Hu W, Shapiro M A. 140-GHz gyrotron experiments based on a confocal cavity [J]. *IEEE Transactions on Plasma ence*, 1998, **26**(3):366-374..
[7] Fu W, Guan X, Yan Y. Harmonic terahertz gyrotron with a double confocal quasi-optical cavity [J]. *Physics of Plasmas*, 2019, **26**(4).
[8] Nusinovich G S. Efficiency of the gyrotron with single and double confocal resonators [J]. *Physics of Plasmas*, 2018, **25**(7):073104.
[9] MEISSNER, Wilh K. Interference spectroscopy. Part I: Erratum [J]. *Journal of the Optical Society of America* (1917-1983), 1942, **32**(4):185-0.
[10] Boyd G D, Kogelnik H. Generalized confocal resonator theory [J]. *Bell Labs Technical Journal*, 1962, **41**(4):1347-1369.
[11] Boyd G D, Gordon J P. Confocal multimode resonator for millimeter through optical wavelength masers [J]. *Bell Labs Technical Journal*, 1961, **40**(2):489-508.
[12] Clark P O. Self-Consistent Field Analysis of Multireflector Optical Resonators [J]. *Journal of Applied Physics*, 1965.